

Research Article

Contribution to the Optimization of the Energy Efficiency of Fixed Collector Panel and Solar Tracking Systems Aimed at Technical-Economic Forecasting

Boaz Wadawa^{1*} , Joseph Yves Effa² , Youssef Errami¹ , Abdellatif Obbadi¹ 

¹Laboratory: Electronics, Instrumentation and Energy, Department of Physical, Faculty of Science, Chouaib Doukkali University, Eljadida, Morocco

²Department of Physics, University of Ngaoundere, P.O. Box 454, Ngaoundere, Cameroon
Email: booz_wadawa@yahoo.fr

Received: 13 March 2024; **Revised:** 7 April 2024; **Accepted:** 17 April 2024

Abstract: The objective of the study is to establish a decision support and design tool that will minimize the costs of installation and maintenance of solar collection systems while guaranteeing efficient performance. To do this, an algorithm is proposed to first determine the solar radiation on a flat surface with optimal inclinations fixed annually, monthly, and seasonally. Then, secondly, to carry out the evaluation of solar radiation using models of one and two-axis solar tracking systems. In addition, a χ^2 homogeneity test tool is proposed to predict the techno-economic profitability of several solar collection systems at the same time. It appears that the capture yield by monthly tilt is higher than approximately 1.2% and 0.2% respectively compared to the annual and seasonal fixed tilt methods. Moreover, the capture rate by dual-axis sun tracking is about 19% and 27% higher than single-axis sun tracking methods and fixed optimal tilt methods respectively. According to the χ^2 test, the two-axis tracking method is the most advantageous from a technical and economic point of view. From the results of the χ^2 test, we can say by analogy that the performances of the TR-axis, IEW-axis, and V-axis models prove to be more profitable than the two-axis model. However, to avoid the practical difficulties linked to the search for technical-economic compromises, some solar field developers prefer the method of fixed capture of the optimal inclination.

Keywords: optimization, technico-economic, solar collection efficiency, inclination, solar tracking, χ^2 test

Nomenclature

β, β_p	Angle of inclination of solar plates relative to the horizontal [°]
T, T_1, T_2, T_3	Linke disorder factor and its auxiliaries
h, θ_z	Height of the sun and height linked to time and the Julian legal day [°]
N, j	Number of the day which characterizes each month of the year
A_h	Seasonal variation
a	Azimuth of the normal to the plane [°]
γ	Height of the normal to the plane ($\gamma = 90 - \beta$) [°]

ω	Hour angle of the sun [°]
θ	Direct incident solar ray received by the plate [°]
S	Direct irradiation by sky on a horizontal plane [w/m ²]
d	Total diffuse irradiation [w/m ²]
B_h	Direct irradiation on the horizontal plane [w/m ²]
G_h	Global radiation on a horizontal plane [w/m ²]
d_i	Diffuse irradiation on an inclined plane [w/m ²]
d_{ri}	Irradiation reflected on an inclined plane [w/m ²]
G	Global radiation incident at a given instant on any plane [w/m ²]
R_b	Direct radiation inclination factor
gne	Radiation outside the atmosphere [w/m ²]
ρ	Albedo of the ground
T	Temperature [°]
RH	Relative Humidity [%]
TSV	True solar time [h]
TL	Legal time given by the watch [h]
GMT	Greenwich Mean Time or Greenwich Mean Time [h]
L, φ, z	Latitude of the location [°]
α_p	Azimuth surface angle [°]
λ	Longitude of the location [decimal degree]
δ, M	Sun declination [°]
i	Angle of incidence [°]
d_1	Diffuse radiation from the sky [w/m ²]
d_2	Diffuse radiation from the ground [w/m ²]
δ_a	Component due to albedo
δ_h	Corresponds to the circle of the horizon
δ_i	Isotropic component
δ_d	Direct component
δ_R	Backscattered component
Q	Amount of lost illuminance [w/m ²]
η	Capture yield [%]
Wc	Useful or captured illuminance [w/m ²]
A	Correlation coefficient [%]
R^2	Determination coefficient [%]
$MAPE$	Mean Absolute Error
X_m, X_{cal}	Measured value and Calculated value
R_α	Rejection zone
$\chi^2_{cal}, \chi^2_{crt}$	Calculated chi-square and Critical chi-square
DOF	Degree of freedom
O_{ij}	Total workforce observed

1. Introduction

The exploitation of solar energy still appears today as a major asset to increasingly more efficiently the energy needs of populations throughout the world. To do this, certain current challenges facing researchers are linked to the development of techniques for optimal capture of solar radiation aim at advantages such as [1]-[4]:

- Increased system performance;
- Reduction in the complexity of implementing optimal techniques;

- Reduction of additional costs linked to optimization, practical implementation, and maintenance of systems;
- Reduction in energy consumption through more sophisticated devices.

Indeed, optimizing the energy efficiency of solar radiation collection systems requires knowing prerequisites such as techniques to adequately increase the solar collection surfaces or solar fields. On the other hand, to look for a good orientation that would allow the surfaces of the panels to always remain perpendicularly exposed to the sun rays [1], [3]. To do this, we focus in this manuscript on the study of the effectiveness of models and the profitability of solar radiation capture systems using solar plates equipped with fixed optimal orientation techniques and/or using tracking devices of the sun. The literature tells us that it has been demonstrated that the energy yields of panels equipped with solar tracking systems can be between 25.76% and 60.10% higher than the yields of horizontally arranged solar collection surfaces [1]. In addition, due to the apparent movement of the sun, it is obvious that a flat surface or fixed collector panel with an optimal inclination is less cost-effective than a collector panel equipped with a sun tracking system. In general, a distinction is made between the category of two-axis sun tracking systems and the category of single-axis tracking systems. To prove the effectiveness of tracking systems on a practical level, work such as that of Yusop et al. [5], Pirayawaraporn et al. [6], Palomino-Resendiz et al. [7], Fatmaryanti et al. [8], Kumar et al. [9], and Obiwulu et al. [10] proposed miniaturized experimental prototypes for small energy production. These single-axis or two-axis tracking prototypes use microcontrollers associated with sensors or without electronic sensors to ensure the positioning of the panels following the apparent movement of the sun. The fundamental differences that exist between these different works are based on criteria such as [5]-[10]:

- The technological choices of the prototypes based on the types of microcontrollers, electronic sensors, motors, filters, and algorithms used;
- The use or not of electronic sensors associated with the microcontroller for tracking the apparent movement of the sun;
- The types of strategies used for maintenance or supervision of monitoring systems;
- The choice of the study site, parameters, and climate measurement data collected;
- Optimization of performance in terms of precision of the envisaged results and reduction of costs.

Generally, the validation of theoretical and practical studies is based on interpretations, observations, and comparisons of results obtained via data collection and/or via the values of statistical performance indicators using data calculated or measured experimentally [1]-[3], [10]. However, theoretical studies aimed at proposing methods for forecasting and evaluating solar radiation in a given location and on fixed solar collection surfaces or based on sun tracking systems, remain essential for the development of solar projects. The main advantages of theoretical methods include:

- Prediction of reliable theoretical data to save time in data collection;
- The development of good specifications or good technical specifications allowing the reduction of costs of practical implementation of solar exploitation projects;
- The production of theoretical results is generally used for the optimization and validation of experimental systems.

Consequently, we can cite the following works: Moumami et al. [11] studied the estimation of solar radiation by the Perrin de Brichambaut model and the method of Liu Jordan. Their studies take into account climatic parameters, local times of day, and fixed inclinations of the solar panels. Unlike Liu Jordan's model, the solar radiation results from Perrin de Brichambaut model present good correlations with the data measured at the Brista site [1], [12], [13]. Chabane et al. [14] developed a theoretical method for calculating global solar radiation on a horizontal surface based on climatic conditions and parameters linked to pollution (CO, CO₂, CH₄, and O₃), and water vapor. We can criticize the model of Chabane et al. for its approximate results (high error rate). In addition, the rarity and the use of several calculation and measurement parameters increase the complexity of using this model. Takilateet al. [15] proposed an empirical model for calculating normal direct solar irradiation (IDN). The latter is a function of the radiation based on the Perrin de Brichambaut model multiplied by the ratios of sunshine and solar radiation involving the sky clarity indices. The results show that the proposed IDN can compete with classical models and models based on intelligent algorithms. Chabane et al. [13] proposed yet another model for predicting global solar radiation on a horizontal collection surface and a fixed inclination surface. This comes from the linear regression method based on the use of the sun positioning equations, daily local time and five arbitrarily chosen tilt angles. The validation of the model of Chabane et al. [13] presented a

good correlation with the measured values and the values of the Perrin de Brichambaut model. Kallioğlu et al. [16] evaluated the capture efficiency of fixed solar panels with optimal inclinations based on the Liu and Jordan model. In addition, they offer a classic economic analysis using standard, prime, and thin-film technology solar modules to improve the financial competition of agri-voltaic systems. Yadav et al. [17] studied the applications of various Artificial Neural Network (ANN) models to evaluate the solar radiation deposit in mountainous areas, in order to predict the power produced by photovoltaic (PV) panels installed with a power of 2,680 Wp. Unlike classic models such as the Liu Jordan and Perrin models, ANN-based models necessarily require practical data for training. In addition, the use of ANNs in another more generalized algorithm like what we are considering may lead to an increase in computational complexity, data processing, and additional costs. In general, the model of two-axis tracking systems is characterized by good adaptability to the movement of the sun, in order to allow good solar collection efficiency and good energy yield. However, the two-axis tracking model also presents a high complexity of design and use compared to single-axis solar tracking models. As a result, most researchers believe that by developing other with increasingly better performance, they will be able to reduce the costs linked to complexity and relatively achieve the performance of two-axis systems. Hence, the fact that we encounter several structures of one-axis systems named as follows [1], [18]:

- Tracking of the NS-axis, rotation around a horizontal axis and positioned in the north-south direction;
- Tracking of the EW-axis, rotation around a horizontal axis and positioned in the east-west direction;
- V-axis tracking, rotation around a vertical axis in a fixed position with optimal inclination;
- IEW-axis tracking, similar to EW-axis tracking, but with an axis of rotation inclined relative to a horizontal surface of optimal inclination;
- Tracking of the TR-axis, or tracking of the inclined rotary axis.

According to the work of Okoye et al. [18], relating to the evaluation of solar radiation based on tracking systems, the results showed that the annual energy yield of the two-axis tracking system is between 1.86% and 31.52% higher than the yields of single-axis tracking systems. In the same vein, Zhu et al. [1] proposed the design of a TR tracking system and the analysis of the performance of tracking systems. The results of the solar radiation evaluations showed that the performance of the two-axis tracking system is superior to (>) TR-axis > IEW-axis > V-axis > EW-axis > NS-axis > the horizontal collection surface.

Furthermore, the study of Khargotra et al. [19] proposed an experimental solar thermal collector (STC) to meet the hot water demand of the population based on the study and economic analysis of good periods of solar activity. However, faced with the complexity of optimal solar monitoring systems, the search for compromises between increases in efficiency and reduction in the cost of collection systems is very essential for the success of a solar collector installation project. To avoid being confronted with the complexity of solar tracking systems, in particular, the constraints linked to the operation, maintenance, and the economic and technical feasibility of the systems. As a result, many researchers will be content to improve the performance offered by fixed solar collection surfaces with optimal inclinations. We can cite scientific work from the oldest to the most recent which is based on the search for methods for calculating optimal inclinations of sensors or fixed solar panels [20]. For Duffie and Beckmann [21], the optimal annual solar capture inclination is equal to the latitude φ of the location. While, depending on the different places of study and observation circles, the expressions of the optimal inclination angles fixed to the year are as follows [20]:

$$\beta_{opt} = \varphi + 20^\circ \quad (1)$$

$$\beta_{opt} = \varphi + 10^\circ \quad (2)$$

$$\beta_{opt} = \arctan \left[\frac{\sum_1^{12} A_{hi} \tan(\varphi + \delta_i)}{\sum_1^{12} A_{hi}} \right] \quad (3)$$

φ , δ_i , and A_{hi} are respectively the latitude of the location, the declination of the sun for the representative day of month (i), and the monthly average per day of global irradiation according to Gladius or direct radiation measured on a horizontal plane according to Kern et al. In addition, studies have been carried out to determine optimal fixed seasonal inclinations (winter and summer), depending on whether the declination of the sun is negative for winter and positive for summer. In practice, the values of these inclinations are specified as being a linear function characterized by the latitude of the location and the average value of the declination characterizing the season considered. Consequently, the following optimal angles were proposed [20]:

For sites located in the Southern Hemisphere,

$$\beta_{opt} = \varphi + 10^\circ \quad (4)$$

For both seasons,

$$\beta_{opt} = \varphi \pm 10^\circ \quad (5)$$

$$\beta_{opt} = \varphi \pm 15^\circ \quad (6)$$

For the different periods of the year, we designate N_1 and N_2 the first and last day over the period considered respectively.

$$\beta_{opt} = \frac{1}{N_2 - N_1 + 1} \sum_{i=N_1}^{N_2} \beta_{opt}(i) \quad (7)$$

Where β_{opt} is the optimal daily angle and can be written according to the latitude of the location; the declination of the sun, and the hour angle as follows:

$$\beta_{opt} = \varphi - \arctan \left[\frac{\omega_s}{\sin \omega_s} \tan \delta(i) \right] \quad (8)$$

ω_s : The hour angle of sunrise.

Later, another analytical model was developed, which makes it possible to determine the fixed optimal tilt angle depending on the latitude of the location and for any day of the year. Then, using the least squares method, he develops correlations making it possible to calculate the optimal fixed angle for each month of the year. These relationships are given as follows [20]:

For the period from January to March:

$$\beta_{opt} = 60.00012 + 1.5Nm + 3.5Nm^2 + (\varphi - 30)(0.7901 + 0.01749Nm + 0.0165Nm^2) \quad (9)$$

For the period from April to June:

$$\beta_{opt} = 216.1 - 72.032219Nm + 6.0031Nm^2 + (\varphi - 40)(1.1 + 0.1124Nm - 0.015035Nm^2) \quad (10)$$

For the period from July to September:

$$\beta_{opt} = 29.11831 - 20.51Nm + 2.502Nm^2 + (\varphi - 50) \left(-11.173 + 2.71Nm - 0.015Nm^2 \right) \quad (11)$$

For the period from October to December:

$$\beta_{opt} = -441.24 + 84.54332Nm - 3.52Nm^2 + (\varphi - 40) \left(4.2137 - 0.5834Nm + 0.0223Nm^2 \right) \quad (12)$$

In these relationships, Nm represents the number of the month.

According to [20], two expressions have been developed to determine the optimal angle of a solar collector facing due south for the use of the collector during heating periods:

$$\beta_{opt} = \arctan \left[M \frac{\cos \delta \sin \omega_s \sin \varphi - \frac{\pi}{180} \omega_s \cos \varphi \sin \delta}{\cos \varphi \cos \delta \sin \omega_s - \frac{\pi}{180} \omega_s \sin \varphi \sin \delta} \right] \quad (13)$$

$$\beta_{opt} = \tan^{-1} \left[M \frac{\tan^2 \varphi \tan \omega_s + \frac{\pi}{180} \omega_s}{\tan \varphi \tan \omega_s - \frac{\pi}{180} \omega_s} \right] \quad (14)$$

Where φ and ω_s are respectively the latitude of the place and the hour angle of sunrise calculated by the following relationship:

$$\omega_s = a \cos[-\tan \varphi \tan \delta] \quad (15)$$

M is the declination of the sun calculated by the relationship proposed by the following expression:

$$M = \pm 2 \left[\frac{B_h / G_h}{1 + B_h / G_h - \rho} \right] \quad (16)$$

B_h , G_h , and ρ are respectively the direct irradiation on the horizontal plane, the overall irradiation on the horizontal plane, and the albedo of the ground of the site considered.

In principle, equations (1) to (16) were developed based on geographical parameters and solar radiation data specific to a given location. Consequently, these equations for calculating optimum angles prove less suitable and ineffective in more generalized applications to the climatic and geographical conditions of other sites. Abdelaal et al. [22] first propose a first algorithm for estimating solar radiation based on the variation in the solar panel inclination angle. Then, the second algorithm is dedicated to determining the optimum angles for which we can capture the maximum possible solar radiation each day, each month, and each season of the year. These two algorithms involve parameters such as declination, the solar constant outside the atmosphere, the angle of sunrise and sunset, the earth-sun distance, and extraterrestrial solar radiation on the horizontal and inclined plane. The values obtained theoretically are in agreement with the experimental values. Indeed, the performance of the fixed capture model with daily inclinations is respectively 1.56% and 7.77% higher than the fixed capture models with one and two annual modifications of the optimal angle. The main drawback of the work of Abdelaal et al. [22] concerns the use in its algorithms of radiation quantities outside the atmosphere, which reduces the consideration of the specific conditions of a given terrestrial location. Therefore, the accuracy of the models they offer is also average and questionable.

Issaq et al. [23] presented the calculations of fixed optimum angles per year, per season, and per month from linear

adjustments of equation models using latitude, declination, clarity indices, and direct solar radiation and diffuse. All things considered in relation to the limits linked to uncertainties, we note that the estimates of solar radiation based on the theoretical models proposed in the literature are in agreement with the data from the sites studied. Indeed, the summary of the work previously cited in the literature concerns:

- Proposals for studies and designs of experimental prototypes for single-axis and two-axis solar tracking consisting of microcontrollers, electronic position sensors, solar tracking algorithms, electronic filters, etc. The measured data, coordinates, and climatic and geographical parameters of the sites are taken into account for the evaluation of solar radiation and the validation of experimental prototypes.

- Studies and proposals for theoretical models for the prediction of solar radiation captured on solar plates equipped with solar tracking devices and on fixed panels arranged horizontally or inclined at optimal angles. Consequently, we retain the Perrin de Brichambaut model for the remainder of our work because it is best suited for the evaluation of solar radiation following all capture modes.

- Analyzes of the advantages linked to energy efficiency and economic profitability of solar monitoring systems [25]. And moreover, several models for calculating the optimal inclination angles of fixed solar collectors are proposed for each day of the months, seasons and year.

However, we note that none of the previously cited works offer prediction models allowing optimal choices of solar capture techniques to be made with good financial returns. Therefore, the optimization of solar collection systems always faces the following main challenges:

- The development of more appropriate tools for the analysis and design of all types of solar energy capture systems;

- The data produced must be reliable, precise, efficient, and adapted for all types of climatic and geographical conditions of terrestrial environments;

- The energy solutions envisaged must present a good compromise between complexity, improved efficiency, and costs.

Considering all the limits and challenges previously listed, we considered a new theoretical approach more appropriate to the optimal exploitation of solar radiation and better suited to all site conditions. Clearly, the proposed approach mainly aims to predict the technical-economic profitability of several solar collection models at the same time. Furthermore, based on technical-economic criteria, the envisaged approach easily allows to do the choice of optimal solar capture methods or techniques among many other existing models. Indeed, optimal choices would be very difficult and almost impossible with traditional approaches to economic studies of systems, particularly when we have a high number of models to choose from. Furthermore, the envisaged approach makes it possible to anticipate effectively the development of good specifications to reduce the costs of practical construction and maintenance of solar collection systems while guaranteeing good energy efficiency. To do this, the approach proposed in this article is detailed in three main parts. The first part is devoted to the methodology as follows:

- Determining the trajectory of the sun from the astronomical equations that govern the characterization of solar radiation on the ground;

- The demonstration of the Perrin de Brichambaut model, which takes into account site conditions for the evaluation of solar radiation on a fixed horizontally or inclined panel, and/or on a solar plate equipped with a monitoring system [1], [25];

- The proposal of a more generalized algorithm making it possible to characterize the evaluation of solar radiation on surfaces of fixed inclination and capture by tracking the sun. In addition, the algorithm designed from astronomical equations and the calculation model of Perrin de Brichambaut also allows the determination of optimum angles of fixed inclination for all days of the year, months, and seasons;

- Modeling the path of the sun through the atmosphere to the ground allows us to assess the capture of solar radiation, in order to deduce the capture efficiency of the panel;

- Demonstration of the application of the χ^2 test, in which we will use the capture efficiency of the solar panel.

The second part is devoted to the results and discussions; this first consists of validating the effectiveness of the proposed approach by determining the degree of correlation that exists between the envisaged results and the results resulting from the proven model of Perrin de Brichambaut. Then, compare the results obtained with the results presented in the literature. Furthermore, the results of the χ^2 test will allow us to predict the technical and economic profitability of

fixed panels and panels equipped with sun-tracking systems.
 The last part is dedicated to the conclusion and perspectives.

2. Methodology

2.1 Model of the path of the sun in relation to a solar collection surface

The solar plate in Figure 1 can be oriented according to the angle of inclination (βp) relative to the horizontal, and located from the angle of the azimuthal surface (αp) and the latitude of location (L). While, solar coordinates depend on the hour angle (ω), and angles such as declination (δ), azimuth (a), height (h), and height (θz) related to time and on the Julian legal day. In addition, (θ) which represents the direct incident solar ray received by the plate is linked to the other angles of Figure 1 by the following three geometric and trigonometric relations [1], [26]:

$$\begin{aligned} \cos(\theta) = & \sin \delta \cos L \cos \beta p - \sin \delta \cos L \sin \beta p \cos \alpha p + \\ & \cos \delta \cos L \cos \beta p \cos \omega + \cos \delta \sin L \sin \beta p \cos \alpha p \cos \omega \end{aligned} \quad (17)$$

$$\cos(\theta) = \cos \theta z \cos \beta p + \sin \theta z \sin \beta p \cos(a - \alpha p) \quad (18)$$

$$\cos(\theta) = \cos \delta \cos \omega \cos(L - \beta p) + \sin \delta \sin(L - \beta p) \quad (19)$$

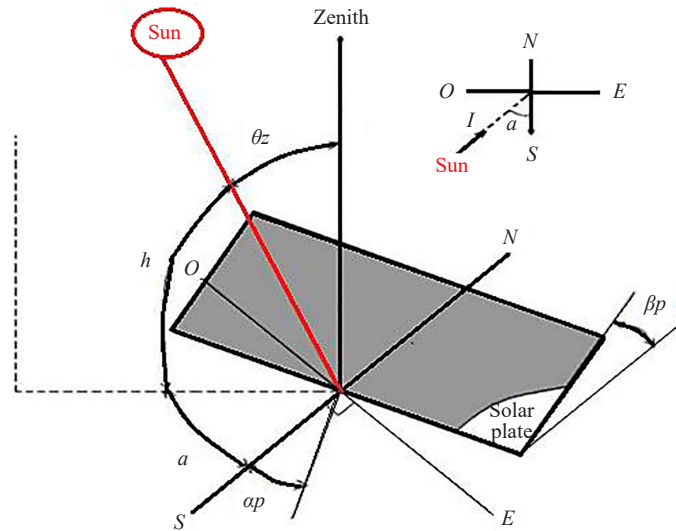


Figure 1. Designation of solar angles on an inclined receiver plate [26]

2.1.1 Equations of the diurnal trajectory of the sun

The mathematical modeling of the trajectory of the sun in its apparent movement consists of locating at any instant the height (h) and azimuth (a) of the sun at any location on the terrestrial globe of latitude (L) and for a day of row (j). By using the resolution of Gauss's equation, we can thus deduce the solar coordinates (h and a) from the following expressions [1]:

$$\sin(h) = \sin L \sin \delta + \cos L \cos \delta \cos \omega \quad (20)$$

$$\sin(a) = \cos \delta \sin \frac{\omega}{\cosh} \quad (21)$$

From Cooper's formula, we calculate the declination (δ), as follows [25]:

$$\delta = 23.45^\circ \sin \left(\frac{360}{365} (j + 284) \right) \quad (22)$$

And, the hour angle (ω) in degrees is obtained [23]:

$$\omega(^{\circ}) = 15^{\circ}(TSV - 12) \quad (23)$$

Where, TSV : Is the true solar time which is obtained by the following expression [1]:

$$TSV = TL - GMT + \left(\frac{Et + 4\lambda}{60} \right) \quad (24)$$

TL represents the legal time given by the watch and λ is the longitude of the location (in decimal degrees). The time correction equation is given by the following formula:

$$Et = 9.87 \sin 2N - 7.35 \cos N - 1.5 \sin N \quad (25)$$

$$N = \frac{360}{365} (j - 81) \quad (26)$$

Where, j is the number of the day which characterizes each month of the year.

For the sake of congestion and errors, instead of varying j from January 1 to 365 days (December 31) or to 366 days of the leap year. We will instead focus on the characteristic number of each month, as defined in Table 1.

Table 1. Characteristic numbers of each month of the year [21]

Month	Jan	Feb	Mar	April	May	Jun	July	Aug	Sep	Oct	Nov	Dec
Day number (j)	0	31	59	90	120	151	181	212	243	273	304	334

2.2 Evaluation of solar radiation on a fixed plane using the Perrin de Brichambaut model

Theoretically, the determination of solar radiation from the Perrin de Brichambaut model takes into account the total Linke haze factor (T) to better characterize the impacts linked to climatic conditions and the geographical coordinates of the place considered.

2.2.1 Linke disorder factor

The Linke disorder factor which allows to better characterize the local climate of a site is defined as the sum of the following three auxiliary disorder factors $T1$, $T2$, and $T3$ [11], [21]:

$$T = T1 + T2 + T3 \quad (27)$$

With,

$$T1 = 2.4 - 0.9 \sin L + 0.1(2 + \sin L)A_h - 0.2L - (1.22 + 0.14A_h)(1 - \sin h) \quad (28)$$

$$T2 = 0.89^L \quad (29)$$

$$T3 = (0.9 + 0.4A_h)0.63^L \quad (30)$$

And the seasonal variation is given by the following relationship:

$$A_h = \sin \left[\frac{360}{365}(N - 121) \right] \quad (31)$$

2.2.2 Direct radiation

For any reception plane, the power of the incident direct radiation is expressed as follows [1], [12], [14], [21]:

$$S = gne \cos \theta \exp \left(- \frac{T}{0.9 + \frac{9.4}{0.89^L} \sin h} \right) \quad (32)$$

The angle of incidence on an inclined plane is given by relation (19). By replacing the relation $\cos(\theta) = \sin(h)$ in equation (32), we will obtain the expression of solar radiation on the horizontal plane as follows [12], [14], [21]:

$$S_h = gne \sin h \exp \left(- \frac{T}{0.9 + \frac{9.4}{0.89^L} \sin h} \right) \quad (33)$$

Where gne denotes the radiation outside the atmosphere given as follows [12]:

$$gne = \left(1 + 0.0334 \cos \left(\frac{360}{365} j - 2 \right) \right) 1353 \quad (34)$$

2.2.3 Diffuse radiation

The total diffuse radiation (d) can be written as follows [11], [12], [21]:

$$d = d_1 + d_2 + d_3 \quad (35)$$

Hence, the diffuse radiation from the sky (d_1) is given as follows:

$$d_1 = \delta_d \cos i + \delta_i \frac{1 + \sin \beta}{2} + \delta_h \cos \beta \quad (36)$$

The direct component (δ_d) is expressed as follows:

$$\delta_d = gne \exp\left(-2.48 + \sin h + ax - \sqrt{4bx^2 + ax^2}\right) \quad (37)$$

Where,

$$ax = 3.1 - 0.4bx \quad (38)$$

$$bx = \log \tau' - 2.28 - 0.50 \log(\sin h) \quad (39)$$

$$\tau' = T1 + T2 \quad (40)$$

The isotropic component (δ_i) which corresponds to a sky of uniform luminance is given as following:

$$\delta_i = d_h - \delta \sin h \quad (41)$$

Where,

$$d_h = gne \exp\left(-1 + 1.06 \log(\sin h) + ay - \sqrt{by^2 + ay^2}\right) \quad (42)$$

$$by = \log \tau' - 2.8 + 1.02(1 - \sin h)^3 \quad (43)$$

$$ay = 1.1 \quad (44)$$

On the other hand, δ_h corresponding to the circle of the horizon, is written:

$$\delta_h = gne \frac{-0.02at}{at^2 + atbt + 1.8} \exp(\sin h) \quad (45)$$

Where, the factors at and bt are given by the following terms:

$$at = \log \tau' - 3.1 \log(\sin h) \quad (46)$$

$$bt = \exp(0.2 + 1.75 \log(\sin h)) \quad (47)$$

Diffuse radiation from the ground (d_2) is given by the following relation:

$$d_2 = \delta_a \frac{1 - \sin \beta}{2} \quad (48)$$

Where, the component (ρ) designates the albedo of the ground, in the following equation:

$$\delta_a = \rho(S_h + d_h) \quad (49)$$

Backscattered diffuse radiation (d_3), is given by the following relation:

$$d_3 = \delta_R \frac{1 + \sin \beta}{2} \quad (50)$$

The term δ_R is given by the following expression:

$$\delta_R = 0.9(\rho - 0.2)(S_h + d_h) \exp\left(\frac{-4}{\sqrt{\tau'}}\right) \quad (51)$$

2.2.4 Global solar radiation

The overall solar radiation incident at a given time and on any plane is defined by the simplified expression G , which designates the sum of the two terms of equations (32) and (35) as follows:

$$G = S + d \quad (52)$$

2.3 Estimation of solar radiation on a flat surface with a two-axis and one-axis tracking system

Tracking system models are based on specific considerations of the symmetry of each direction considered for tracking the apparent trajectory of the sun.

2.3.1 Two-axis tracking system

The two-axis tracking device is a system with two degrees of freedom according to which the angle of incidence of the sun's rays must correspond 100% to the normal of the receiving plane of the solar panel. To do this, the simplified expression of the angle of incidence in the Perrin de Brichambaut model must be replaced by the term $\cos(\theta) = 1$ in equation (18), and to deduce the following relationships [1], [18]:

$$\begin{cases} \beta p = \theta z \\ \alpha p = a \end{cases} \quad (53)$$

2.4 Tracking system with one axis or one degree of freedom

The positioning of the solar plate can follow an optimal fixed monthly, annual, or seasonal inclination, facing due south towards the equator, as illustrated in Figure 2. Furthermore, the one-axis tracking device which caught our

attention obeys the positioning in Figure 2, whose solar collection surface is here equipped with a solar tracking device with one degree of freedom in the direction from East to West (azimuthal tracking). We choose this type of so-called EW-axis tracking system to better study overall and by extrapolation the technical-economic profitability of single-axis tracking techniques such as TR-axis, IEW-axis, and V-axis [1], [18].

For an axis-EW tracking model, one can use the following consideration:

$$\cos \theta = \sin(h + \beta p) \tag{54}$$

The condition of equation (54) is true if and only if the parameters θz and αp of equation simplify (18) obey the following equalities [1], [18]:

$$\begin{cases} \theta z = \beta p = 90 - h \\ \alpha p = a \end{cases} \tag{55}$$

2.5 Algorithm for calculating the optimal tilt angle for a fixed solar plate or one equipped with a single-axis tracking system

The steps described in sections 2.1, 2.2, and 2.3 are brought together in the algorithm in Figure 3 to initially characterize the evaluation of solar radiation on surfaces of fixed inclination and collection by tracking the sun. Manipulation of the algorithm first makes it possible to determine optimal fixed tilt angles for all days of the year, months and seasons. Using the assumptions of equation (53) in equation (52) of the Perrin de Brichambaut model, we then run the algorithm after declaring as input the climatic and geographical parameters of the place considered. As indicated in Figure 3, for each month of the year, for a length of day, and for all angles ranging from 0° to 90°, the corresponding global solar radiation is determined. Consequently, the angle which will correspond to the maximum radiation captured (E_{max}) during the year, month or season, will be called optimal angle (β_{opt}). The second manipulation of the algorithm consists first of using the assumptions of equations (54) and (55) in equation (52) respectively for the one-axis and two-axis solar tracking, and then isolate the loop calculates the angles in the algorithm in Figure 3. By rolling out the algorithm for each case of solar tracking, we determine the average solar radiation results corresponding to each month of the year.

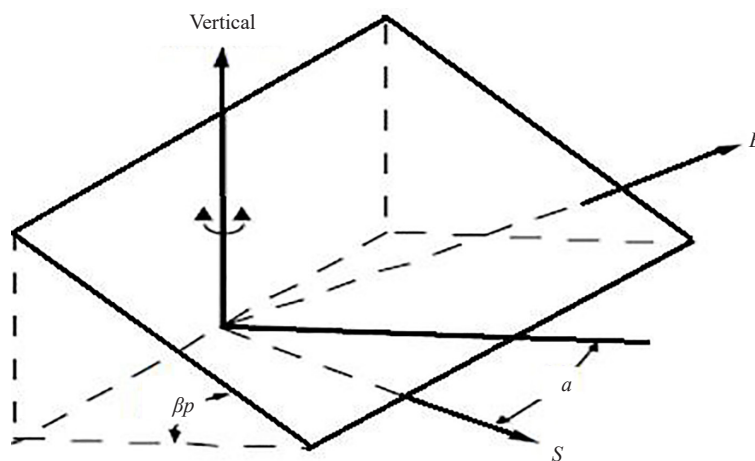


Figure 2. Indication of axis of rotation and optimal inclination of solar plane equipped with single-axis tracking

the following relation:

$$\eta(\%) = \frac{\text{Useful or captured illuminance } (W_c)}{\text{Illumination received or available } (W_f)} \quad (56)$$

By transposing this relationship into our case study, we can write the expression for the illumination received or available as follows:

$$W_f = \sum_{i=1}^{12} \overline{gne(i)} \quad (57)$$

With, $\langle gne \rangle$ is the average radiation outside the atmosphere for each characteristic day number j . The useful or captured illuminance will correspond to the following notation:

$$W_c = \overline{G(j)} \quad (58)$$

Where, $\langle G(j) \rangle$ represents the global average radiation for each characteristic day number j . Additionally, the term (Q) in Figure 4 corresponds to the lost illumination which brings together all the losses linked to the positioning of the panel and the climatic, orographic, and geographical conditions of the given location.

2.7 Statistical indicators to evaluate the performance of a prediction model

In general, we encounter several types of statistical performance indicators to validate a prediction model. The main indicators most used in our case study are as follows.

2.7.1 Correlation coefficient R

The criterion states that if the correlation coefficient noted R is very close to the value 1, we can say that the values predicted by the calculation model and those obtained by measurements go in the same direction, and are very close to each other. The expression for R is as follows [21], [27]:

$$R = \frac{\frac{1}{N} \sum_{i=1}^N (X_m^i - \overline{X_m}) (X_{cal}^i - \overline{X_{cal}})}{\sqrt{\frac{1}{N} \sum_{i=1}^N (X_m^i - \overline{X_m})^2} \sqrt{\frac{1}{N} \sum_{i=1}^N (X_{cal}^i - \overline{X_{cal}})^2}} \quad (59)$$

X_m : the measured value; X_{cal} : the calculated value.

2.7.2 Coefficient of determination

The criterion of the coefficient of determination denoted R^2 . For $0 < R^2 < 1$, we can clearly appreciate the dispersion of the measured values around the curve of the prediction model. The coefficient of determination is calculated as follows [18], [23]:

$$R^2 = 1 - \frac{\sum_{i=1}^N (X_m^i - X_{cal}^i)^2}{\sum_{i=1}^N (X_m^i - \overline{X_m})^2} \quad (60)$$

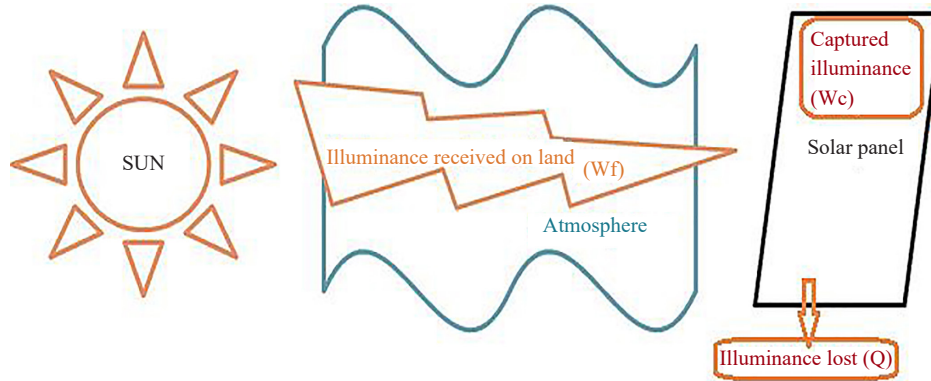


Figure 4. Energy balance of the path of the sun illumination through the atmosphere to the solar plate

2.7.3 Mean Absolute Percentage Error (MAPE)

The mean absolute percentage error (MAPE) makes it possible to determine the uncertainty between the measured values and the calculated values, as follows [21], [27]:

$$MAPE = \frac{100}{N} \sum_{i=1}^N \left| \frac{X_m^i - X_{cal}^i}{X_m^i} \right| \quad (61)$$

2.8 The chi-square test

In principle, there are three types of χ^2 test which vary according to questions or subjective sampling hypotheses, as follows [28]:

- The χ^2 adequacy test is based on the Null hypothesis (Ho), such as “Does the character of the variable X follow a particular law?”;
- The χ^2 test of homogeneity, defined by the Ho hypothesis, such as “Does the character X follow the same law in two or more groups of given populations?”;
- The χ^2 Independence test, for Ho: “Are the characters X and Y independent?”.

The χ^2 test for homogeneity will attract our attention for the simple reason that it will help us to determine whether the distribution of the panel efficiencies or collection rates is the same across the categories of fixed solar collectors and solar panels with tracking systems. However, these three tests obey the same principles of problem formulation. We divide the observations into K classes, the numbers of which are noted, N_1, \dots, N_k . Then, we calculate the theoretical numbers, denoted $n, th \dots nk, th$ as follows:

$$n_{ij}, th = O_i O_j / O \quad (62)$$

With, O_i, O_j , and O are respectively the elements of the i th row, the j th column, and the total O of all the elements in a table of observed numbers.

The test expression is:

$$U = \sum_{I=1}^K \frac{(N_i - n_{i, th})^2}{n_{i, th}} \quad (63)$$

Furthermore, the statistics that we have defined theoretically can also follow the law table or abacus, using the

following relationship:

$$U \approx \chi^2(k-1-m) \tag{64}$$

Where k is the number of classes and m is the number of parameters estimated necessary to calculate the theoretical numbers.

Then, we calculate the unilateral rejection zone noted, $R\alpha \in [t\alpha, +\infty)$, by choosing a tolerance threshold α for which we determine the critical limit $t\alpha$ in the law table or chart. Therefore, we can define the following decision rules:

- If U does not belong to $R\alpha$, we accept H_0 in our case study.
- Otherwise, we reject H_0 .

3. Results and discussions

Based on the methodological approach presented previously, the results obtained can be described in three main stages, namely. The first step concerns Table 2 which summarizes the results of the evaluation of solar radiation captured by a fixed flat surface of optimal inclinations per year, per month and per season. Columns 1, 2, and 3 of Table 2 respectively denotes the months of the year, the number of the day (j) which characterizes each month of the year, and the values $\langle g_{ne} \rangle$ of the average monthly intensity of illumination received by the earth also called average radiation values outside the atmosphere. The elements of columns 4 [29] and 5 of Table 2 allows to determine the following statistical performance indicators: $R^2 = 0.9850$, $R = 0.9931$, $MEA = 4.1189$. We can be note that there is a good correlation between the measured solar radiation values and the calculated values. Furthermore, the results obtained with the proposed approach are as well correlated with the measured values as with the results of the work presented in the literature [1], [2], [11], [18], [22], [29]. Therefore, this allows us to validate the choice and effectiveness of the Perrin de Brichambaut model which is used in the optimization algorithm proposed in Figure 3. From the results of the algorithm in Figure 3, we obtain the curves of Figures 5, 6, and 7 of the maximum daily solar radiation (between sunrise and sunset), as well as the optimal tilt angles corresponding to each day of the months, seasons, and year, respectively.

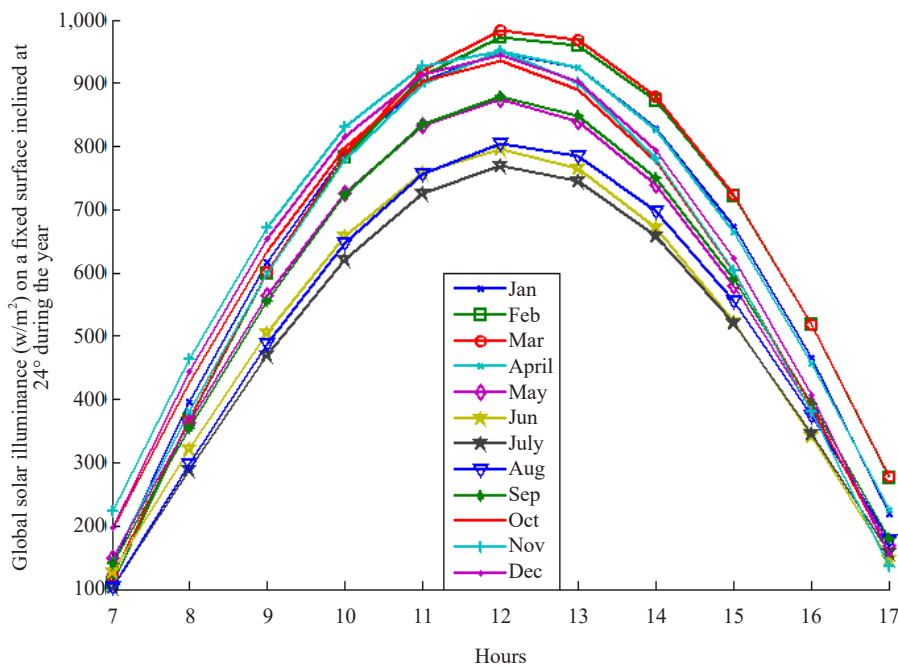


Figure 5. Maximum solar radiation collected each day on a fixed solar plate with an optimal inclination of 24° throughout the year

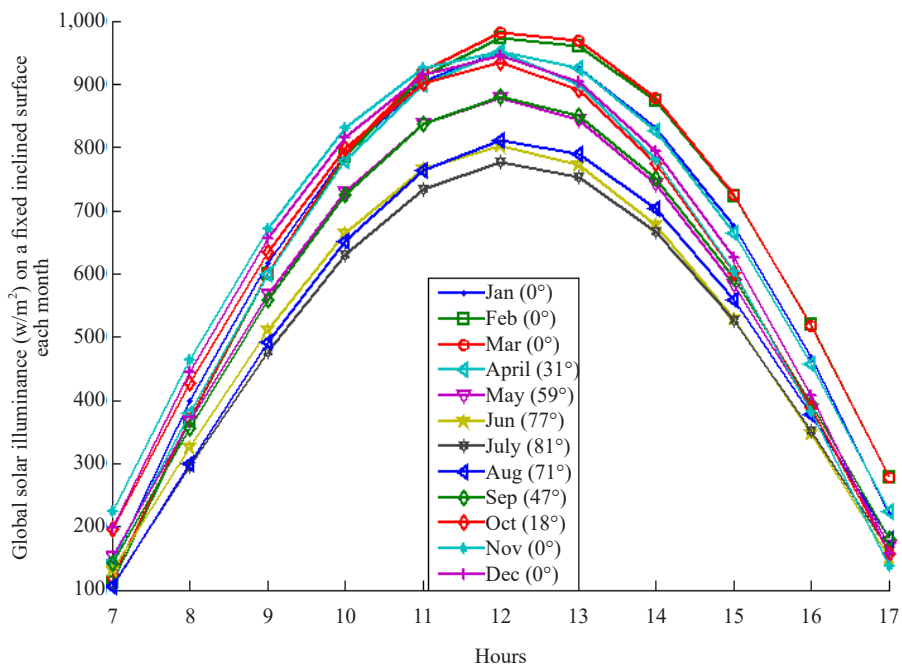


Figure 6. Maximum solar radiation collected each day on a fixed solar plate with optimal monthly inclinations

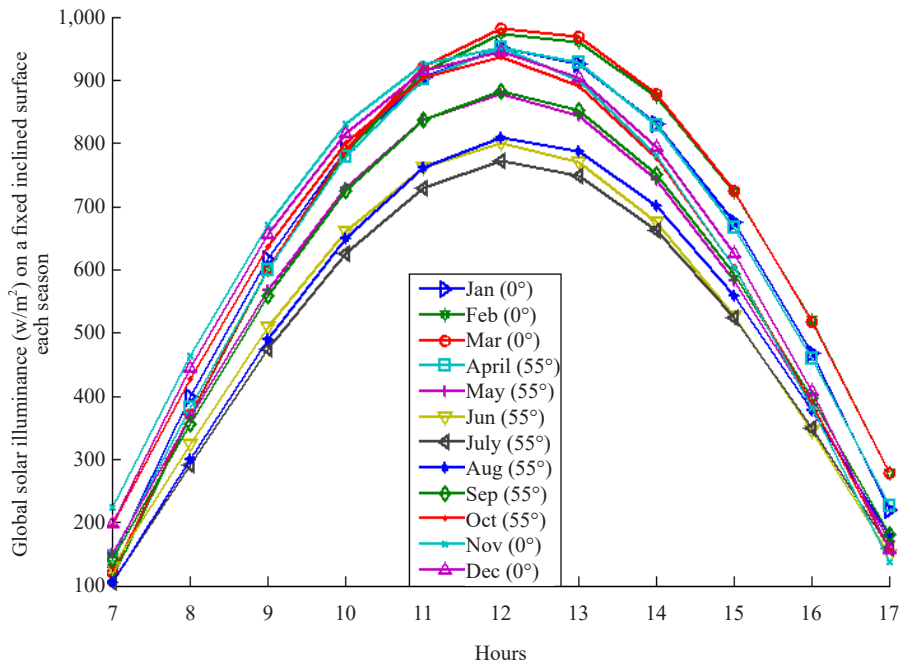


Figure 7. Maximum solar radiation collected each day on a fixed solar plate with optimal seasonal inclinations

In Table 2, columns 5, 6, and 7 represent respectively the monthly averages of maximum illuminances ($G(W/m^2)$) and the optimum angles (β_{opt}) correspond for fixed inclinations per year, per month and per season. In addition, W_f represents the annual sum of the monthly average irradiance and $\eta(\%)$, is the capture efficiency or annual average yield

of the solar panel. We see that the monthly capture yield, which requires an adjustment of the inclination every month, is higher by approximately 0.2% and 1.2% compared to seasonal and annual solar capture respectively. The seasonal yield is approximately 1% above the annual tilt yield. Furthermore, these different yield gaps that we obtain are in agreement with the performance range of fixed capture models predicted in the work of Abdelaal et al. [22]. In addition, the curves obtained in Figures 6 and 7 are in agreement with the performances and morphologies of the curves exposed in works [2], [11], [14], [29]. However, a statistical study of techno-economic forecasting is necessary to objectively conclude that the capture models can or cannot offer and achieve the same compromise in terms of maintenance, cost and performance.

Table 2. Summary of the results obtained as part of the study of optimal solar caption methods using the fixed inclination of flat sensors

Month	j	$\langle gne \rangle$ (W/m ²)	Solar Radiation on the Horizontal Plane		Annual	Monthly		Seasonal	
			Measure [29] G_m (W/m ²)	Calculated G (W/m ²)	G (W/m ²) $\beta_{opt} = 24^\circ$	β_{opt} (°)	G (W/m ²)	β_{opt} (°)	G (W/m ²)
Jan	0	1,240.1	441	369.6	628	0	629.20	0	629.20
Feb	31	1,235.2	492.1	397	644.73	0	645.53	0	645.53
Mar	59	1,222.3	487	437.5	650.33	0	650.31	0	650.31
April	90	1,202.3	492.2	474.3	622.61	31	622.95	55	624.08
May	120	1,182.2	471.3	486	565.63	59	568.67	55	568.33
Jun	151	1,166.4	446.1	481	510.12	77	515.91	55	513.52
July	181	1,160	434	477.5	491.36	81	497.76	55	494.86
Aug	212	1,164.3	394	480	516.68	71	512.30	55	519.74
Sep	243	1,178.6	463	479	568.17	47	569.73	55	570.30
Oct	273	1,198.1	457	458	609.61	18	609.45	55	610.41
Nov	304	1,218.7	479.1	416	624.15	0	624.51	0	624.51
Dec	334	1,233.8	443	379.4	622.73	0	623.77	0	623.77
Total		1,4402	5,499.8	5,335.3	7,054.12		7,070.09		7,074.6
Yield η (%)		100	38.2%	37.05%	48.8%		50%		49.8

The second stage, dedicated to Table 3, summarizes the results of the evaluation of solar radiation collected on a solar collection surface equipped based on one-axis and two-axis monitoring models. By associating Perrin de Brichambaut model with the equations of the apparent trajectory of the sun, we obtain the daily maximum solar radiation (between sunrise and sunset) for the one-axis and two-axis tracking models respectively as shown in Figures 8 and 9.

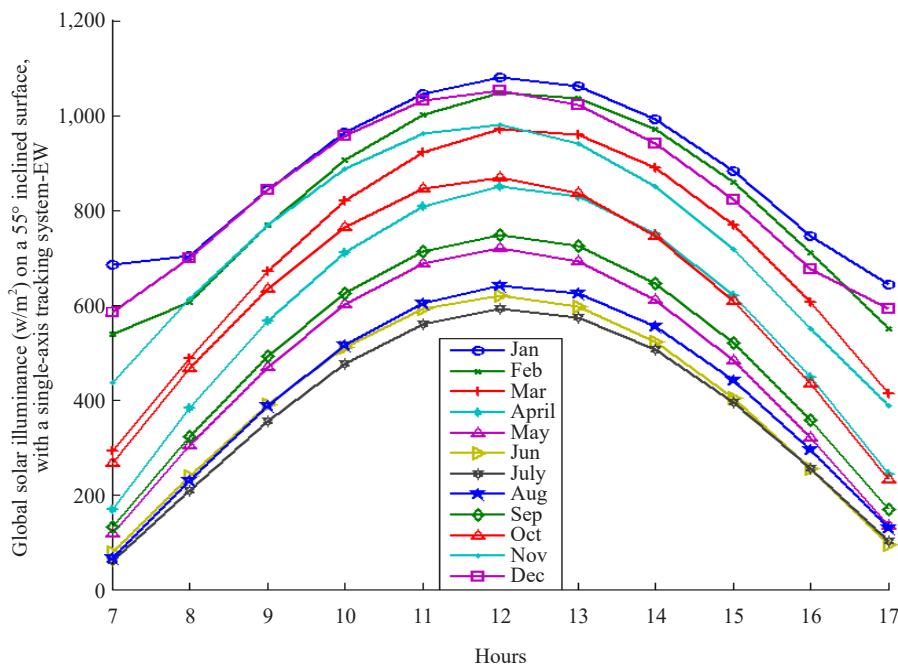


Figure 8. Maximum solar radiation collected per day on a solar plate with optimal inclinations of 55° based on a one-axis tracking system

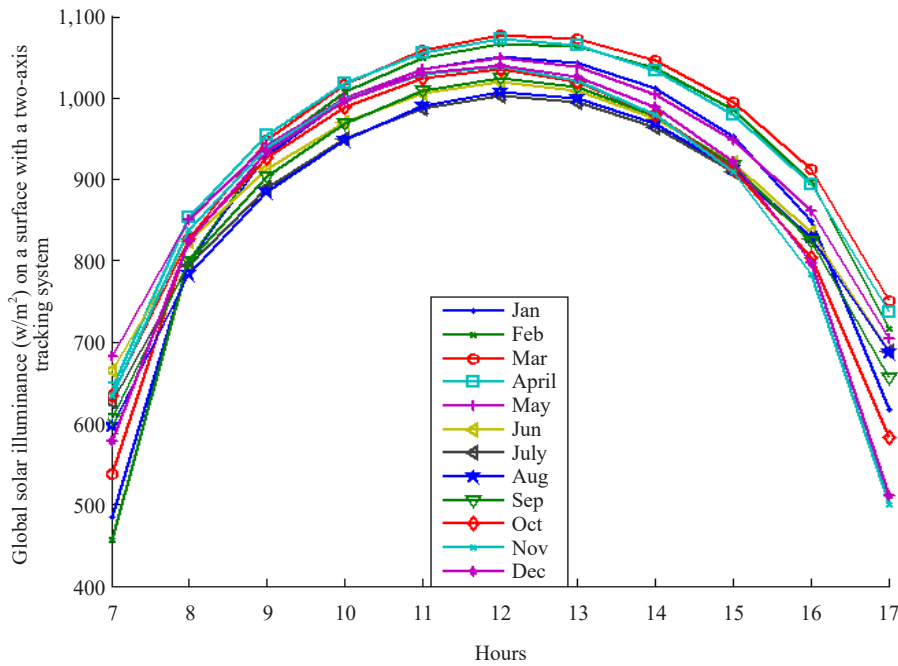


Figure 9. Maximum solar radiation collected per day on a solar plate with a two-track tracking system

Columns 4 and 5 of Table 3 represent monthly averages of illuminances based on one-axis and two-axis tracking methods. We also note that the capture efficiency by two-axis tracking is approximately 19% higher than the capture efficiency by single-axis tracking. This value 19% we obtained is initially in agreement with the range of performances

which show the superiority of two-axis tracking models over the performance of horizontal capture models predicted in the literature [1], [2], [18].

Table 3. Summary of evaluation of solar radiation captured based on one-axis and two-axis tracking methods

Month	j	$\langle g_{ne} \rangle$ (W/m ²)	For single-axis tracking at $\beta_{opt} = 55^\circ$, G (W/m ²)	For two-axis tracking, G (W/m ²)
Jan	0	1,240.1	961.89	888.31
Feb	31	1,235.2	897.77	910.47
Mar	59	1,222.3	780.16	931.27
April	90	1,202.3	638.74	936.83
May	120	1,182.2	515.70	919.70
Jun	151	1,166.4	432.18	893.27
July	181	1,160	410.12	875.70
Aug	212	1,164.3	450.50	873.38
Sep	243	1,178.6	545.99	881.47
Oct	273	1,198.1	670.65	884.84
Nov	304	1,218.7	808.31	879
Dec	334	1,233.8	920.11	877.40
Total		14,402	8,032.11	10,751.64
Yield η (%)		100	55.77%	74.65%

Table 4. Statistical interpretation of the illumination rate captured over a year by the one-axis and two-axis tracking methods

Tracking capture methods	Illumination rate captured	Illumination rate lost	Total
One-axis	56	44	100
Two-axis	75	25	100
Total	131	69	200

Secondly, this efficiency of 19% belongs to the interval in which the two-axis tracking model is better than the one-axis tracking models described in the work [1]. However, statistical forecasting for techno-economic decision-making is also necessary. The third step aims to apply the χ^2 test to determine whether or not there is homogeneity between the capture yields of the methods presented in Tables 2 and 3. To do this, let us consider the initial hypotheses at a tolerance threshold of 0.05, as follows:

Ho: The distribution of capture rates or correlation returns is the same or is homogeneous;

H1: The distribution of capture rates or correlation returns is not the same or not homogeneous.

The formulation of the test consists first of determining the observed numbers in Tables 4 and 5 in order to respectively deduce the calculated Khy2 (χ^2 cal).

Table 5. Statistical interpretation of the illumination rate captured over a year using fixed inclination capture methods

Capture methods by fixed	Illumination rate captured	Illumination rate lost	Total
Annual	48.8	51.2	100
Monthly	50	50	100
Seasonal	49.8	50.2	100
Total	148.6	151.4	300

From the formulation of our test in section G, we determine the theoretical numbers (n_{ij} , th) contained in Tables 6 and 7. Then, we use the values of the degrees of freedom (DOF) from Tables 6 and 7 to determine in Table 8, the theoretical or critical χ^2 at a tolerance threshold of 5%.

Table 6. Illumination rate theoretically captured over a year based on one-axis and two-axis tracking methods

Tracking capture methods	Illumination rate captured	Illumination rate lost	Total
One-axis	65.5	34.5	100
Two-axis	65.5	34.5	100
Total	131	69	200

Table 7. Illumination rate theoretically captured all year round by a fixed solar plate and optimal annual, monthly, and seasonal inclinations

Capture methods by fixed optimal inclination	Illumination rate captured	Illumination rate lost	Total
Annual	49.53	50.5	100
Monthly	49.53	50.5	100
Seasonal	49.53	50.5	100
Total	148.56	151.4	300

In Table 8, we determine the χ^2 cal and the χ^2 crt for each of the two capture methods by tracking and by fixed optimal inclinations. The results in Table 8 for solar capture by tracking show firstly that $\chi^2_{cal} > \chi^2_{crt}$, which leads us to say that the Ho hypothesis is rejected. Consequently, there is no homogeneity between the yields of single-axis and

two-axis tracking methods. In other words, the two-axis tracking technique will prove to be more profitable from a technical and economic point of view than the single-axis sun tracking method. The second case in Table 8 concerning the capture models by fixed orientations shows that $\chi^2_{cal} < \chi^2_{crit}$, hence the H_0 hypothesis is accepted. Specifically, we say that there is homogeneity or the distribution of capture rates or yields of different methods identical during each year at the tolerance threshold of 5%. Consequently, from a technical and economic point of view, we can say that the capture method by fixed optimal inclination (24°) all year round is more advantageous than monthly and seasonal captures. Overall, the two-axis tracking method presents a great technical and economic advantage with an efficiency of approximately 28% higher than the fixed capture and single-axis tracking methods. By analogy, if we stick to the results of the work of [1] and [2], the performance of the one-axis tracking models TR-axis, IEW-axis, and V-axis is around 0.2% and 2% closer to the performance of the two-axis tracking model. Therefore, the χ^2 test allows us to assert that the single-axis tracking models (TR-axis, IEW-axis, and V-axis) prove to be more profitable than the two-axis tracking model. Furthermore, to avoid the difficulties linked to the technical complexity of implementation, maintenance, and additional costs, the collection technique by fixed optimal orientation all year round is often more common, particularly in solar fields.

Table 8. Values of $\chi^2_{cal(calculated)}$, $\chi^2_{crit(critical)}$, and degrees of freedom (*DOF*) of the optimal tracking and fixed inclination capture methods

Calculation	Tracking capture method	Fixed optimal tilt capture method
$\chi^2_{cal(calculated)}$	7.88	0.033
Degree of freedom (<i>DOF</i>)	1	2
$\chi^2_{crit(critical)}$	3.84	5.99

4. Conclusion

The main objective of this study is to contribute to the rational exploitation of the solar resource graciously offered by nature. This concerns the proposal of an optimization algorithm allowing solar panels to capture the maximum possible solar irradiation at lower costs. More precisely, the proposed algorithm makes it possible to first determine the solar radiation on a flat surface with optimal inclinations fixed annually, monthly, and seasonally. Then, secondly, evaluate solar radiation using models of one- and two-axis solar tracking systems. Furthermore, a statistical analysis of the χ^2 homogeneity test is proposed to predict the techno-economic profitability of several solar collection systems at the same time. For a case study, we use geographic coordinates and solar radiation data samples collected in 2014 in the Maoura region in the far north of Cameroon. It appears that the solar capture efficiency by monthly inclinations is higher by approximately 1.2% and 0.2% compared to the annual and seasonal fixed inclination methods respectively. In contrast, the capture rate by two-axis solar tracking is approximately 19% and 28% higher than the yields of single-axis and fixed optimal inclinations solar tracking methods, respectively. The χ^2 test allows us to affirm that the two-axis tracking method is the most advantageous from a technical and economic point of view. However, by analogy with the results obtained from the χ^2 test, we can still say that the performances of the single models, TR-axis, IEW-axis, and V-axis, are approximately 0.2% and 2% very close to the performances of the two-axis solar tracking model. This proves a homogeneity of performance, which leads us to conclude that the single-axis models prove to be more cost-effective than the two-axis solar tracking model. However, to avoid the practical difficulties linked to the search for the techno-economic stability of the systems, the collection method by optimal inclination fixed annually constitutes an alternative for solar field projects. In perspective, we plan to implement a software which will integrate the entire proposed approach of our study and can be associated with an emulator or an experimental test bench that will allow a good prediction study and practical validation of the effectiveness or the technical and economic profitability of several solar collection methods at the same time.

Data availability statement

All of the information and resources produced during the work are included in this research article.

Conflict of interest

The authors declare no competing financial interest.

References

- [1] Y. Q. Zhu, J. H. Liu, and X. H. Yang, "Design and performance analysis of a solar tracking system with a novel single-axis tracking structure to maximize energy collection," *Applied Energy*, vol. 264, pp. 114647, 2020. Available: <https://doi.org/10.1016/j.apenergy.2020.114647>.
- [2] T. Demirdelen, H. Alici, B. Esenboğa, and M. Güldürek, "Performance and economic analysis of designed different solar tracking systems for mediterranean climate," *Energies*, vol. 16, no. 10, pp. 4197, 2023. Available: <https://doi.org/10.3390/en16104197>.
- [3] B. Hammad, A. AL-Sardeah, M. Al-Abed, S. Nijmeh, and A. Al-Ghandoor, "Performance and economic comparison of fixed and tracking photovoltaic systems in Jordan," *Renewable and Sustainable Energy Reviews*, vol. 80, pp. 827-839, 2017. Available: <https://doi.org/10.1016/j.rser.2017.05.241>.
- [4] A. Afzal, A. Buradi, M. Alwetaishi, U. Ağbulut, B. Kim, H. G. Kim, and S. G. Park, "Single-and combined-source typical metrological year solar energy data modelling," *Journal of Thermal Analysis and Calorimetry*, vol. 148, no. 22, pp. 12501-12523, 2023. Available: <https://doi.org/10.1007/s10973-023-12604-4>.
- [5] A. Yusop, M. A. S. B. M. Shabri, N. A. Sulaiman, K. N. Khamil, R. Mohammed, and J. M. Sultan, "Development and evaluation of dual axis solar tracking system with iot data monitoring," *Przegląd Elektrotechniczny*, vol. 99, no. 1, pp. 28-32, 2023. Available: <https://doi.org/10.15199/48.2023.01.05>.
- [6] A. Pirayawaraporn, S. Sappaniran, S. Nooraksa, C. Prommai, N. Chindakham, and C. Jamroen, "Innovative sensorless dual-axis solar tracking system using particle filter," *Applied Energy*, vol. 338, pp. 120946, 2023. Available: <https://doi.org/10.1016/j.apenergy.2023.120946>.
- [7] S. I. Palomino-Resendiz, F. A. Ortiz-Martínez, I. V. Paramo-Ortega, J. M. González-Lira, and D. A. Flores-Hernández, "Optimal selection of the control strategy for dual-axis solar tracking systems," *IEEE Access*, vol. 11, pp. 56561-56573, 2023. Available: <https://doi.org/10.1109/ACCESS.2023.3283336>.
- [8] S. D. Fatmaryanti, Y. A. Hakim, and U. Pratiwi, "Design of laboratory scale dual axis solar tracking system with digital converter of light intensity," *AIP Conference Proceedings*, vol. 2706, no. 1, pp. 020094, 2023. Available: <https://doi.org/10.1063/5.0120632>.
- [9] M. D. Kumar, T. M. Kumar, K. Akshay, S. Y. Kumar, and U. Vikas, "Dual axis solar tracking system," *International Journal of Applied Power Engineering*, vol. 12, no. 4, pp. 391-398, 2023. Available: <https://doi.org/10.11591/ijape.v12.i4.pp391-39>.
- [10] A. U. Obiwulu, N. Erusiafe, M. A. Olopade, and S. C. Nwokolo, "Modeling and estimation of the optimal tilt angle, maximum incident solar radiation, and global radiation index of the photovoltaic system," *Heliyon*, vol. 8, no. 6, pp. E09598, 2022. Available: <https://doi.org/10.1016/j.heliyon.2022.e09598>.
- [11] A. Moumami, N. Hamani, N. Moumami, and Z. Mokhtari, *Estimation du rayonnement solaire par deux approches semi empiriques dans le site de Biskra [Two semi-empirical methods were used to estimate the solar radiation at Biskra station]*. 8th International Symposium on Energy Physics, Beshar, Algeria, 2006.
- [12] I. Rougab, M. Reguigue, and A. Cheknane, "Contribution to the forecasting and estimation of solar radiation components at ground level in Algeria," *Romanian Journal of Information Technology and Automatic Control*, vol. 33, no. 1, pp. 43-56, 2023. Available: <https://doi.org/10.33436/v33i1y202304>.
- [13] F. Chabane, F. Guellai, M.-Y. Michraoui, D. Bensahal, A. Bima, and N. Moumami, "Prediction of the global solar radiation on inclined area," *Applied Solar Energy*, vol. 55, pp. 41-47, 2019. Available: <https://doi.org/10.3103/S0003701X19010055>.
- [14] F. Chabane, N. Moumami, C. Toumi, S. Boulouf, and A. Hecini, "Theoretical study of global solar radiation on horizontal area for determination of direct and diffuse solar radiation," *Iranian Journal of Energy and Environment*, vol. 14, no. 1, pp. 9-16, 2023. Available: <https://doi.org/10.5829/ijee.2023.14.01.02>.

- [15] A. Takilalte, A. Dali, M. Laissaoui, and A. Bouhallassa, "Prediction of direct normal irradiation using a new empirical sunshine duration-based model," *Journal of Renewable Energies*, vol. 26, no. 1, pp. 91-103, 2023. Available: <https://doi.org/10.54966/jreen.v26i1.1119>.
- [16] M. A. Kallioğlu, A. S. Avcı, A. Sharma, R. Khargotra, and T. Singh, "Solar collector tilt angle optimization for agrivoltaic systems," *Case Studies in Thermal Engineering*, vol. 54, pp. 103998, 2024. Available: <https://doi.org/10.1016/j.csite.2024.103998>.
- [17] A. K. Yadav, R. Khargotra, D. Lee, R. Kumar, and T. Singh, "Novel applications of various neural network models for prediction of photovoltaic system power under outdoor condition of mountainous region," *Sustainable Energy, Grids and Networks*, vol. 38, pp. 101318, 2024. Available: <https://doi.org/10.1016/j.segan.2024.101318>.
- [18] C. O. Okoye, A. Bahrami, and U. Atikol, "Evaluating the solar resource potential on different tracking surfaces in Nigeria," *Renewable and Sustainable Energy Reviews*, vol. 81, pp. 1569-1581, 2018. Available: <https://doi.org/10.1016/j.rser.2017.05.235>.
- [19] R. Khargotra, R. Kumar, A. Kovács, and T. Singh, "Techno-economic analysis of solar thermal collector for sustainable built environment," *Journal of Thermal Analysis and Calorimetry*, vol. 149, no. 3, pp. 1175-1184, 2024. Available: <https://doi.org/10.1007/s10973-023-12775-0>.
- [20] M. Koussa, A. Malek, and M. Haddadi, "Apport énergétique de la poursuite solaire sur deux axes par rapport aux systèmes fixes. Application aux capteurs plans [Compared to fixed systems, solar energy pursues the energy contribution on both axes. Applications of planar sensors]," *Journal of Renewable Energies*, vol. 10, no. 4, pp. 515-537, 2007.
- [21] J. A. Duffie, W. A. Beckman, and N. Blair, *Solar Engineering of Thermal Processes, Photovoltaics and Wind*. Wiley, 2020.
- [22] A. K. Abdelaal, and A. El-Fergany, "Estimation of optimal tilt angles for photovoltaic panels in Egypt with experimental verifications," *Scientific Reports*, vol. 13, no. 1, pp. 3268, 2023. Available: <https://doi.org/10.1038/s41598-023-30375-8>.
- [23] S. Z. Issaq, S. K. Talal, and A. A. Azooz, "Empirical modeling of optimum tilt angle for flat solar collectors and PV panels," *Environmental Science and Pollution Research*, vol. 30, no. 33, pp. 81250-81266, 2023. Available: <https://doi.org/10.1007/s11356-023-28142-3>.
- [24] H. Zarei Zohdi, and M. Sarvi, "Optimal and economic evaluation of using a two-axis solar tracking system in photovoltaic power plants, a case study of "Tehran", Iran," *Journal of Solar Energy Research*, vol. 8, no. 1, pp. 1211-1221, 2023. Available: <https://doi.org/20.1001.1.25883097.2023.8.1.1.7>.
- [25] T. M. Yunus Khan, M. E. M. Soudagar, M. Kanchan, A. Afzal, N. R. Banapurmath, N. Akram, S. D. Mane, and K. Shahapurkar, "Optimum location and influence of tilt angle on performance of solar PV panels," *Journal of Thermal Analysis and Calorimetry*, vol. 141, pp. 511-532, 2020. Available: <https://doi.org/10.1007/s10973-019-09089-5>.
- [26] H. Djalo, and P. Njampou, "Modèle de Gassara dans la poursuite de la production pic d'une plaque solaire par régulation de deux degrés de liberté [The Gasala model pursues the peak generation of the solar plate by adjusting two degrees of freedom]," *Journal of Renewable Energies*, vol. 16, no. 4, pp. 749-759, 2013.
- [27] D. Y. Goswami, *Principles of Solar Engineering*. Boca Raton: CRC press, 2022. Available: <https://doi.org/10.1201/9781003244387>.
- [28] N. S. Turhan, "Karl Pearson's chi-square tests," *Educational Research and Reviews*, vol. 16, no. 9, pp. 575-580, 2020. Available: <https://doi.org/10.5897/ERR2019.3817>.
- [29] C. T. Fotsing, D. Njomo, C. Cornet, P. Dubuisson, and J. L. Nsouandele, "Acquisition and study of global solar radiation in Maroua-Cameroon," *International Journal of Renewable Energy Research*, vol. 5, no. 3, pp. 910-918, 2015. Available: <https://dergipark.org.tr/en/download/article-file/148047>.